

The Fairness of Risk Scores Beyond Classification: Bipartite Ranking and the xAUC Metric

Nathan Kallus*^{1,2} and Angela Zhou†^{1,2}

¹School of Operations Research and Information Engineering, Cornell University

²Cornell Tech, Cornell University

Abstract

Where machine-learned predictive risk scores inform high-stakes decisions, such as bail and sentencing in criminal justice, fairness has been a serious concern. Recent work has characterized the disparate impact that such risk scores can have when used for a binary classification task and provided tools to audit and adjust resulting classifiers. This may not account, however, for the more diverse downstream uses of risk scores and their non-binary nature. To better account for this, in this paper, we investigate the fairness of predictive risk scores from the point of view of a bipartite ranking task, where one seeks to rank positive examples higher than negative ones. We introduce the xAUC disparity as a metric to assess the disparate impact of risk scores and define it as the difference in the probabilities of ranking a random positive example from one protected group above a negative one from another group and vice versa. We provide a decomposition of bipartite ranking loss into components that involve the discrepancy and components that involve pure predictive ability within each group. We further provide an interpretation of the xAUC discrepancy in terms of resource allocation fairness and make connections to existing fairness metrics and adjustments. We assess xAUC empirically on datasets in recidivism prediction, income prediction, and cardiac arrest prediction, where it describes disparities that are not evident from simply comparing within-group predictive performance.

1 Introduction

Predictive risk scores support decision-making in high-stakes settings such as bail sentencing in the criminal justice system, triage and preventive care in healthcare, and lending decisions in the credit industry [36, 2]. In these areas where predictive errors can significantly impact individuals involved, studies of fairness in machine learning have analyzed the possible disparate impact introduced by predictive risk scores primarily in a *binary classification setting*: if predictions determine whether or not someone is detained pre-trial, is admitted into critical care, or is extended a loan. But the “human in the loop” with risk assessment tools often has recourse to make decisions about extent, intensity, or prioritization of resources. That is, in practice, predictive risk scores are used to provide informative rank-orderings of individuals with binary outcomes in the following settings:

- (1) In criminal justice, the “risk-needs-responsivity” model emphasizes matching the level of social service interventions to the specific individual’s risk of re-offending [5, 3]. Cowgill [16] finds quasi-experimental evidence of judges increasing bail amounts for marginal candidates at low/medium risk thresholds, suggesting that judges informed by the COMPAS risk scores vary the intensity of bail.

*kallus@cornell.edu

†az434@cornell.edu

- (2) In healthcare and other clinical decision-making settings, risk scores are used as decision aids for prevention of chronic disease or triage of health resources, where a variety of interventional resource intensities are available [37, 28, 36, 8].
- (3) In credit, predictions of default risk affect not only loan acceptance/rejection decisions, but also risk-based setting of interest rates. Fuster et al. [22] embed machine-learned credit scores in an economic pricing model which suggests negative economic welfare impacts on Black and Hispanic borrowers.
- (4) In municipal services, predictive analytics tools have been used to direct resources for maintenance, repair, or inspection by prioritizing or bipartite ranking by risk of failure or contamination [38, 10]. Proposals to use new data sources such as 311 data, which incur the self-selection bias of citizen complaints, may introduce inequities in resource allocation [30].

We describe how the problem of *bipartite ranking*, that of finding a good ranking function that ranks positively labeled examples above negative examples, better encapsulates how predictive risk scores are used in practice to rank individual units, and how a new metric we propose, xAUC, can assess ranking disparities.

Most previous work on fairness in machine learning has emphasized disparate impact in terms of confusion matrix metrics such as true positive rates and false positive rates and other desiderata, such as probability calibration of risk scores. Due in part to inherent trade-offs between these performance criteria, some have recommended to retain *unadjusted* risk scores that achieve good calibration, rather than adjusting for parity across groups, in order to retain as much information as possible and allow human experts to make the final decision [12, 9, 27, 13]. At the same time, unlike other regression-based settings, group-level discrepancies in the *prediction loss* of risk scores, relative to the true Bayes-optimal score, are not observable, since only binary outcomes are observed.

Our bipartite ranking-based perspective illuminates a gap between the differing arguments made by ProPublica and Equivant (then Northpointe) regarding the potential bias or disparate impact of the COMPAS recidivism tool. Equivant claims fairness of the risk scores due to calibration, within-group AUC parity (“accuracy equity”), and predictive parity in response to ProPublica’s allegations of bias due to true positive rate/false positive rate disparities for the Low/Not Low risk labels [2, 18]. Our xAUC metrics shed light on assessing the *across-group* accuracy inequities (xAUC) and ranking error disparities that may be introduced by a potential risk score.

In this paper, we propose and study the cross-ROC curve and the corresponding xAUC metric for assessing disparities induced by a predictive risk score, as they are used in broader contexts to inform resource allocation. We relate the xAUC metric to different group- and outcome-based decompositions of a *bipartite ranking* loss, which emphasizes the importance of assessing *cross-group* accuracy equity beyond just within-group accuracy equity, and assess the resulting metrics on datasets where fairness has been of concern.

2 Related Work

Our analysis of fairness properties of risk scores in this work is most closely related to the study of “disparate impact” in machine learning, which focuses on disparities in the *outcomes* of a process across protected classes, without racial animus [4]. Many previous approaches have considered formalizations of disparate impact in a binary classification setting [33, 41, 25]. Focus on disparate impact differs from the study of questions of “individual fairness”, which emphasizes the “similar treatment of similar individuals” [19].

Previously considered methods for fairness in binary classification assess group-level disparities in confusion matrix-based metrics. Proposals for error rate balance assess or try to equalize true positive rates and/or false positive rates, error rates measured conditional on the *true* outcome, emphasizing the equitable treatment of those who actually are of the outcome type of interest [25, 41]. Alternatively, one might assess the negative/positive predictive value (NPV/PPV) error rates conditional on the thresholded *model prediction* [11].

The predominant criterion used for assessing fairness of *risk scores*, outside of a binary classification setting, is that of calibration. Group-wise calibration requires that

$$\Pr[Y = 1 \mid R = r, A = a] = \Pr[Y = 1 \mid R = r, A = b] = r,$$

as in [11]. The impossibilities of satisfying notions of error rate balance and calibration simultaneously have been discussed in [29, 11]. Liu et al. [31] show that group calibration is a byproduct of unconstrained empirical risk minimization, and therefore is not a restrictive notion of fairness. Hebert-Johnson et al. [26] note the critique that group calibration does not restrict the *variance* of a risk score as an unbiased estimator of the Bayes-optimal score.

Other work has considered fairness in ranking settings specifically, with particular attention to applications in information retrieval, such as questions of fair representation in search engine results. Yang and Stoyanovich [40] assess statistical parity at discrete cut-points of a ranking, incorporating position bias inspired by normalized discounted cumulative gain (nDCG) metrics. Celis et al. [7] consider the question of fairness in rankings, where fairness is considered as constraints on diversity of group membership in the top k rankings, for any choice of k . Singh and Joachims [39] consider fairness of exposure in rankings under known relevance scores and propose an algorithmic framework that produces probabilistic rankings satisfying fairness constraints in expectation on exposure, under a position bias model. We focus instead on the bipartite ranking setting, where the area under the curve (AUC) loss emphasizes ranking quality on the entire distribution, whereas other ranking metrics such as nDCG or top- k metrics emphasize only a portion of the distribution.

The problem of bipartite ranking is related to, but distinct from, binary classification [20, 34, 1]. While the bipartite ranking induced by the Bayes-optimal score is analogously Bayes-risk optimal for bipartite ranking (*e.g.*, [32]), in general, a probability-calibrated classifier is not optimizing for the bipartite ranking loss. Cortes and Mohri [15] observe that AUC may vary widely for the same error rate, and that algorithms designed to globally optimize the AUC perform better than optimizing surrogates of the AUC or error rate. Narasimhan and Agarwal [35] study transfer regret bounds between the related problems of binary classification, bipartite ranking, and outcome-probability estimation.

3 Problem Set-up and Notation

We suppose we have data (X, A, Y) on features $X \in \mathcal{X}$, sensitive attribute $A \in \mathcal{A}$, and binary labeled outcome $Y \in \{0, 1\}$. We are interested in assessing the downstream impacts of a predictive risk score $R : \mathcal{X} \times \mathcal{A} \rightarrow \mathbb{R}$, which may or may not access the sensitive attribute. When these risk scores represent an estimated conditional probability of positive label, $R : \mathcal{X} \times \mathcal{A} \rightarrow [0, 1]$. For brevity, we also let $R = R(X, A)$ be the random variable corresponding to an individual’s risk score. We generally use the conventions that $Y = 1$ is associated with opportunity or benefit for the individual (*e.g.*, freedom from suspicion of recidivism, creditworthiness) and that when discussing two groups, $A = a$ and $A = b$, the group $A = a$ might be a historically disadvantaged group.

Let the conditional cumulative distribution function of the learned score R evaluated at a threshold θ given label and attribute be denoted by

$$F_y^a(\theta) = \Pr[R \leq \theta \mid Y = y, A = a].$$

We let $G_y^a = 1 - F_y^a$ denote the complement of F_y^a . We drop the a subscript to refer to the whole population: $F_y(\theta) = \Pr[R \leq \theta \mid Y = y]$. Thresholding the score yields a binary classifier, $\hat{Y}_\theta = \mathbb{I}[R \geq \theta]$. The classifier’s true negative rate (TNR) is $F_0(\theta)$, its false positive rate (FPR) is $G_0(\theta)$, its false negative rate (FNR) is $F_1(\theta)$, and its true positive rate (TPR) is $G_1(\theta)$. Given a risk score, the choice of optimal threshold for a binary classifier depends on the differing costs of false positive and false negatives. We might expect cost ratios of false positives and false negatives to differ if we consider the use of risk scores to direct punitive measures or to direct interventional resources.

In the setting of bipartite ranking, the data comprises of a pool of positive labeled examples, $S_+ = \{X_i\}_{i \in [m]}$, drawn i.i.d. according to a distribution $X_+ \sim D_+$, and negative labeled examples $S_- = \{X_i\}_{i \in [n]}$

drawn according to a distribution $X_- \sim D_-$ [34]. The true rank order is determined by a *preference function* $f : \mathcal{X} \times \mathcal{X} \rightarrow \{-1, 0, 1\}$ which describes the preference ordering of pairs of instances (X, X') : $f(X, X') = +1$ if X' is preferred to X , $f(X, X') = -1$ if X is preferred to X' , and $f(X, X') = 0$ if X and X' have the same ranking; this can be extended to a stochastic setting. The bipartite ranking problem is a specialization where the goal is to find a score function that ranks positive examples above negative examples with good generalization error, corresponding to the following true preference function:

$$f(X, X') = \begin{cases} 1 & X' \in S_+, X \in S_- \\ -1 & X' \in S_-, X \in S_+ \\ 0 & \text{o.w.} \end{cases}$$

The rank order may be determined by a score function $s(X)$, which achieves empirical bipartite ranking error $\frac{1}{mn} \sum_{i=1}^m \sum_{j=1}^n \mathbb{I}[s(X_i) < s(X_j)]$.

The area under the receiver operating characteristic (ROC) curve (AUC), a common (reward) objective for bipartite ranking is often used as a metric describing the quality of a predictive score, independently of the final threshold used to implement a classifier, and is invariant to different base rates of the outcomes. The ROC curve plots $G^0(\theta)$ on the x-axis with $G^1(\theta)$ on the y-axis as we vary θ over the space of various decision thresholds. The AUC is the area under the ROC curve, *i.e.*,

$$\text{AUC} = \int_0^1 G_1(G_0^{-1}(v))dv$$

An AUC of $\frac{1}{2}$ corresponds to a completely random classifier; therefore, the difference from $\frac{1}{2}$ serves as a metric for the diagnostic quality of a predictive score. We recall the probabilistic interpretation of AUC that it is the probability that a randomly drawn example from the positive class is correctly ranked by the score R above a randomly drawn score from the negative class [24].

Lemma 1 (Probabilistic interpretation of the AUC). *Let R_1 be drawn from $R | Y = 1$ and R_0 be drawn from $R | Y = 0$ independently. Then*

$$\text{AUC} = \Pr[R_1 > R_0]$$

It has been noted that the estimate for the AUC is the same as the estimate for the Mann-Whitney U-statistic, and therefore also closely related to the nonparametric Wilcoxon rank-sum test for differences between distributions [14, 24]. The corresponding null hypothesis of $\Pr[R_1 > R_0] = \frac{1}{2}$ is a necessary condition of distributional equivalence with the observation that $\int F(s)df(s) = \frac{1}{2}$. Other representations of the AUC are studied in Menon and Williamson [32]; we focus on its use as an accuracy metric for bipartite ranking.

4 The Cross-ROC and Cross-Area Under the Curve (xAUC) metric

We introduce the cross-ROC curve and the cross-area under the curve metric xAUC that summarize group-level disparities in *misranking* errors induced by a score function $R(X, A)$.

Definition 1 (Cross-Receiver Operating Characteristic curve (xROC)).

$$\begin{aligned} \text{xROC}(\theta; R, a, b) \\ = (\Pr[R > \theta | A = b, Y = 0], \Pr[R > \theta | A = a, Y = 1]) \end{aligned}$$

The $\text{xROC}^{a,b}$ curve parametrically plots $\text{xROC}(\theta; R, a, b)$ over the space of thresholds $\theta \in \mathbb{R}$, generating the curve of TPR of group a on the y-axis vs. the FPR of group b on the x-axis. We define the $\text{xAUC}(a, b)$ metric as the area under the $\text{xROC}^{a,b}$ curve.

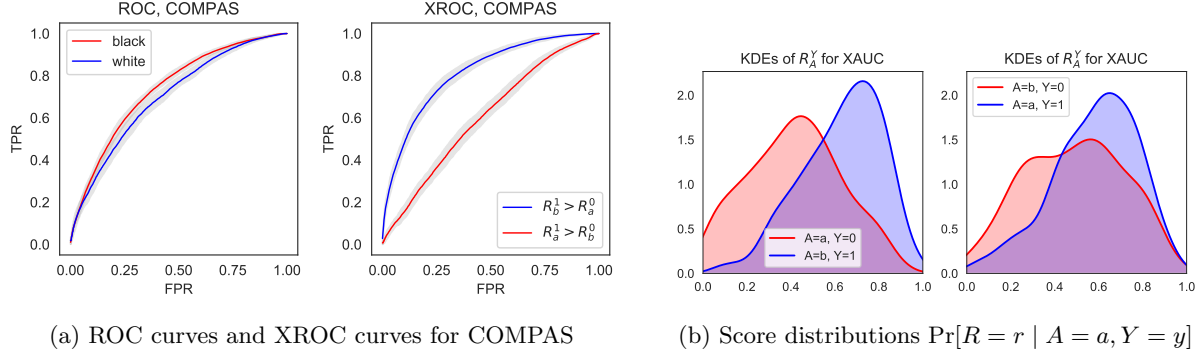


Figure 1: Analysis of xAUC disparities for the COMPAS Violent Recidivism Prediction dataset

Definition 2 (xAUC).

$$\text{xAUC}(a, b) = \int_0^1 G_1^a((G_0^b)^{-1}(v)) dv$$

Analogous to the usual AUC, we provide a probabilistic interpretation of the xAUC metric as the probability of correctly ranking a positive instance of group a above a negative instance of group a under the corresponding outcome- and class-conditional distributions of the score.

Lemma 2 (Probabilistic interpretation of xAUC).

$$\text{xAUC}(a, b) = \Pr[R_1^a > R_0^b]$$

where R_1^a is drawn from $R | Y = 1, A = a$ and R_0^b is drawn from $R | Y = 0, A = b$ independently. For brevity, henceforth, R_y^a is taken to be drawn from $R | Y = y, A = a$ and independently of any other such variable. We also drop the subscript to denote omitting the conditioning on sensitive attribute (*e.g.*, R_y).

The xAUC accuracy metrics for a binary sensitive attribute measure the probability that a randomly chosen unit from the “positive” group $Y = 1$ in group a , is ranked higher than a randomly chosen unit from the “negative” group, $Y = 0$ in group b , under the corresponding group- and outcome-conditional distributions of scores R_y^a . We let AUC^a denote the *within-group* AUC for group $A = a$, $\Pr[R_1^a > R_0^a]$.

If the difference between these metrics, the xAUC disparity

$$\Delta \text{xAUC} = \Pr[R_1^a > R_0^b] - \Pr[R_1^b > R_0^a]$$

is substantial and negative, then we might consider group b to be “advantaged” in some sense when $Y = 1$ is a positive label or outcome or associated with greater beneficial resources, and “disadvantaged” if $Y = 1$ is a negative or harmful label or is associated with punitive measures. When higher scores are associated with opportunity or additional benefits and resources, Group b either gains by correctly having its deserving members correctly ranked above the non-deserving members of group a , or by having its non-deserving members incorrectly ranked above the deserving members of group a . The magnitude of the disparity describes the misranking disparities incurred under this predictive score, while the magnitude of the xAUC measures this particular across-subgroup rank-accuracy.

Computing the xAUC is simple: one simply computes the sample statistic, $\frac{1}{n_0^b n_1^a} \sum_{i: \substack{A_i=a, \\ Y_i=1}} \sum_{j: \substack{A_j=b, \\ Y_j=0}} \mathbb{I}[R(X_i) > R(X_j)]$. Algorithmic routines for computing the AUC quickly by a sorting routine can be directly used to compute the xAUCs.

Variants of the xAUC metric We can decompose AUC differently and assess different variants of the xAUC:

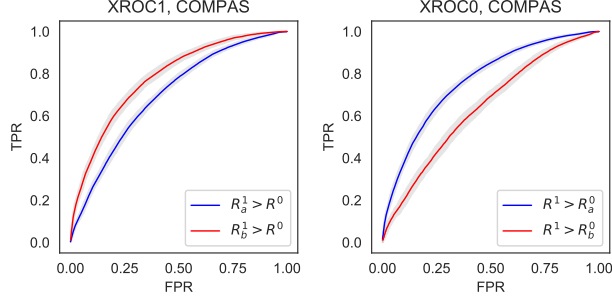


Figure 2: Balanced xROC curves for COMPAS

Definition 3 (Balanced xAUC).

$$\begin{aligned} \text{xAUC}_0(a) &= \Pr[R_1 > R_0^a], \quad \text{xAUC}^0(b) = \Pr[R_1 > R_0^b] \\ \text{xAUC}^1(a) &= \Pr[R_1^a > R_0], \quad \text{xAUC}^1(b) = \Pr[R_1^b > R_0] \end{aligned}$$

These xAUC disparities compare misranking error faced by individuals from either group, conditional on a specific outcome: $\text{xAUC}_0(a) - \text{xAUC}^0(b)$ compares the ranking accuracy faced by those of the negative class $Y = 0$ across groups, and $\text{xAUC}^1(a) - \text{xAUC}^1(b)$ analogously compares those of the positive class $Y = 1$.

xAUC metrics as decompositions of AUC The following proposition shows how the population AUC decomposes as weighted combinations of the xAUC and within-class AUCs, or the balanced decompositions xAUC_1 or xAUC_0 , weighted by the outcome-conditional class probabilities.

Proposition 3.

$$\begin{aligned} \text{AUC} &= \Pr[R_1 > R_0] \\ &= \sum_{b' \in \mathcal{A}} \Pr[A = b' \mid Y = 0] \sum_{a' \in \mathcal{A}} \Pr[A = a' \mid Y = 1] \Pr[R_1^{a'} > R_0^{b'}] \\ &= \sum_{a' \in \mathcal{A}} \Pr[A = a' \mid Y = 1] \Pr[R_1^{a'} > R_0] \\ &= \sum_{a' \in \mathcal{A}} \Pr[A = a' \mid Y = 0] \Pr[R_1 > R_0^{a'}] \end{aligned}$$

5 Assessing xAUC

5.1 COMPAS Example

In Fig. 1, we revisit the COMPAS data and assess our xROC and xAUC curves to illustrate ranking disparities that may be induced by risk scores learned from this data. The COMPAS dataset is of size $n = 6167$, $p = 402$, where sensitive attribute is race, with $A = a, b$ for black and white, respectively. We define the outcome $Y = 1$ for non-recidivism within 2 years and $Y = 0$ for violent recidivism. Covariates include information on number of prior arrests and age; we follow the pre-processing of Friedler et al. [21].

We first train a logistic regression model on the original covariate data (we do not use the decile scores directly in order to do a more fine-grained analysis), using a 70%, 30% train-test split and evaluating metrics on the out-of-sample test set. In Table 1, we report the group-level AUC and the Brier [6] scores (summarizing

Table 1: Ranking error metrics (AUC, xAUC, Brier scores for calibration) for different datasets. We include standard errors in Table 3 of the appendix.

		COMPAS		Framingham		German		Adult	
$A =$		a	b	a	b	a	b	a	b
Logistic Reg.	AUC	0.737	0.701	0.768	0.768	0.726	0.788	0.923	0.898
	Brier	0.208	0.21	0.201	0.166	0.211	0.158	0.075	0.111
	XAUC	0.604	0.813	0.795	0.737	0.708	0.802	0.865	0.944
	XAUC ¹	0.698	0.781	0.785	0.756	0.712	0.791	0.874	0.905
	XAUC ⁰	0.766	0.641	0.755	0.783	0.79	0.775	0.943	0.895
RankBoost cal.	AUC	0.745	0.703	0.789	0.797	0.704	0.796	0.924	0.899
	Brier	0.206	0.21	0.182	0.15	0.22	0.158	0.074	0.109
	XAUC	0.599	0.827	0.822	0.761	0.714	0.788	0.875	0.941
	XAUC ¹	0.702	0.79	0.809	0.783	0.711	0.793	0.882	0.906
	XAUC ⁰	0.776	0.638	0.777	0.811	0.774	0.783	0.939	0.897

calibration), and our xAUC metrics. The xAUC for column $A = a$ is $\text{xAUC}(a, b)$, for column $A = b$ it is $\text{xAUC}(b, a)$, and for column $A = a$, xAUC^y is $\text{xAUC}^y(a)$. The Brier score for a probabilistic prediction of a binary outcome is $\frac{1}{n} \sum_i (R(X_i) - Y_i)^2$. The score is overall well-calibrated (as well as calibrated by group), consistent with analyses elsewhere [11, 18].

We also report the metrics from using a bipartite ranking algorithm, Bipartite Rankboost of Freund et al. [20] and calibrating the resulting ranking score by Platt Scaling, displaying the results as “RankBoost cal.” We observe essentially similar performance across these metrics, suggesting that the behavior of xAUC disparities is independent of model specification or complexity; and that methods which directly optimize the population xAUC error may still incur these group-level error disparities.

In Fig. 1a, we plot ROC curves and our xROC curves, displaying the averaged ROC curve (interpolated to a fine grid of FPR values) over 50 sampled train-test splits, with 1 standard error bar shaded in gray. We include standard errors in Table 3 of the appendix. While a simple *within-group* AUC comparison suggests that the score is overall more accurate for blacks – in fact, the AUC is slightly higher for the black population with $\text{AUC}^a = 0.737$ and $\text{AUC}^b = 0.701$ – computing our xROC curve and xAUC metric shows that blacks would be disadvantaged by misranking errors. The cross-group accuracy $\text{xAUC}(a, b) = 0.604$ is significantly lower than $\text{xAUC}(b, a) = 0.813$: black innocents are nearly indistinguishable from actually guilty whites. This ΔxAUC gap of -0.21 is precisely the **cross-group accuracy inequity** that simply comparing *within-group AUC* does not capture. When we plot kernel density estimates of the score distributions in Fig. 1b from a representative training-test split, we see that indeed the distribution of scores for black innocents $\Pr[R = r \mid A = a, Y = 0]$ has significant overlap with the distribution of scores for white innocents.

Assessing balanced xROC: In Fig. 2, we compare the $\text{xROC}_0(a), \text{xROC}_0(b)$ curves with the $\text{xROC}_1(a), \text{xROC}_1(b)$ curves for the COMPAS data. The relative magnitude of ΔxAUC_1 and ΔxAUC_0 provides insight on whether the burden of the xAUC disparity falls on those who are innocent or guilty. Here, since the ΔxAUC_0 disparity is larger in absolute terms, it seems that misranking errors result in inordinate benefit of the doubt in the errors of distinguishing risky whites ($Y = 0$) from innocent individuals, rather than disparities arising from distinguishing innocent members of either group from generally guilty individuals.

5.2 Assessing xAUC on other datasets

Additionally in Fig. 3 and Table. 1, we evaluate these metrics on multiple datasets where fairness may be of concern, including risk scores learnt on the Framingham study, the German credit dataset, and the Adult

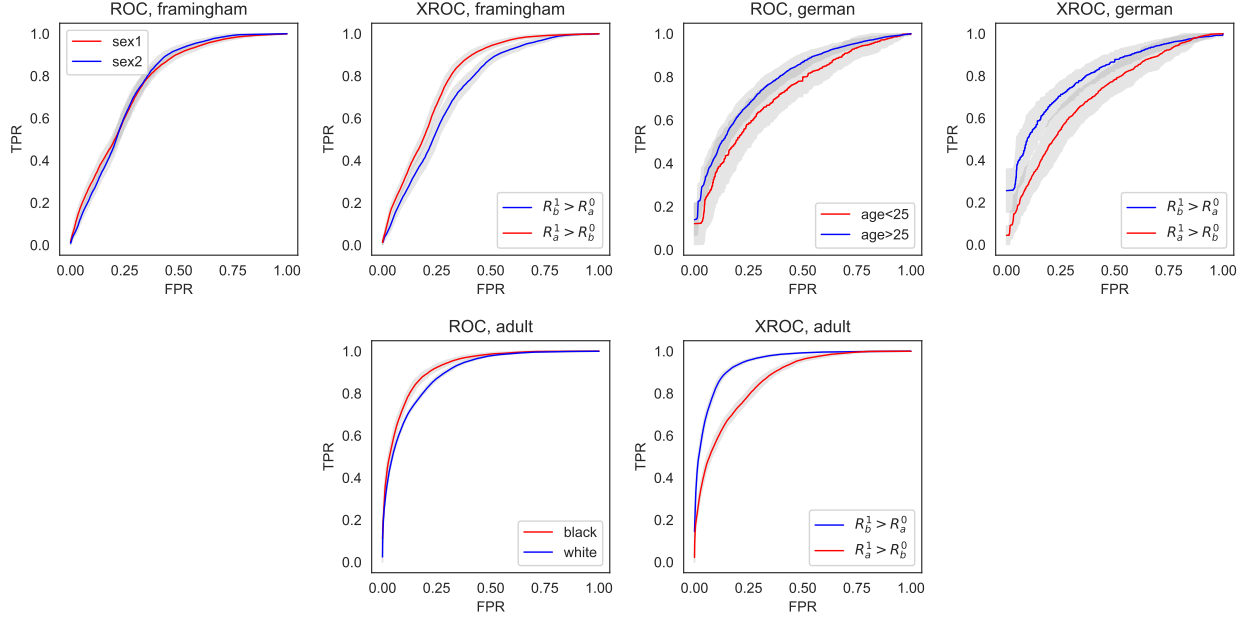


Figure 3: ROC and xROC curve comparison for Framingham, German credit, and Adult datasets.

income prediction dataset (we use logistic regression as well as calibrated bipartite RankBoost) [? 17]. For the Framingham dataset (cardiac arrest risk scores), $n = 4658, p = 7$ with sensitive attribute of gender, $A = a$ for male and $A = b$ for female. $Y = 1$ denotes 10-year coronary heart disease (CHD) incidence. Fairness considerations might arise if predictions of likelier mortality are associated with greater resources for preventive care or triage. The German credit dataset is of size $n = 1000, p = 57$, where the sensitive attribute is age with $A = a, b$ for age < 25 , age > 25 . Creditworthiness (non-default) is denoted by $Y = 1$, and default by $Y = 0$. The “Adult” income dataset is of size $n = 30162, p = 98$, sensitive attribute, $A = a, b$ for black and white. We use the dichotomized outcome $Y = 1$ for high income $> 50k$, $Y = 0$ for low income $< 50k$.

Overall, Fig. 3 shows that these xAUC disparities persist, though the disparities are largest for the COMPAS and the large Adult dataset. For the Adult dataset this disparity could result in the misranking of poor whites above wealthy blacks; this could be interpreted as possibly inequitable withholding of economic opportunity from actually-high-income blacks. The additional datasets also display different phenomena regarding the score distributions and $xROC_0, xROC_1$ comparisons, which we include in Fig. 6 of the Appendix.

6 Properties of the xAUC metric

We proceed to characterize the xAUC metric and its interpretations as a measure of cross-group ranking accuracy. For a perfect classifier with $AUC = 1$, the xAUC metrics are also 1. For a classifier that classifies completely at random achieving $AUC = 0.5$, the xAUCs are also 0.5. Notably, the xROC implicitly compares performance of thresholds that are the same for different levels of the sensitive attribute, a restriction which tends to hold in applications under legal constraints regulating disparate treatment.

For the sake of example we can assume normally distributed risk scores within each group and outcome condition and re-express the AUC in terms of the cdf of the convolution of the score distributions. For $R_0^a \sim N(\mu_{a0}, \sigma_{a0}^2), R_1^b \sim N(\mu_{b1}, \sigma_{b1}^2)$, (drawn independently, conditional on outcome $Y = 1, Y = 0$),

$$\Pr[R_1^a > R_0^b] = \Phi\left(\frac{\mu_{b0} - \mu_{a1}}{\sqrt{\sigma_{a1}^2 + \sigma_{b0}^2}}\right)$$

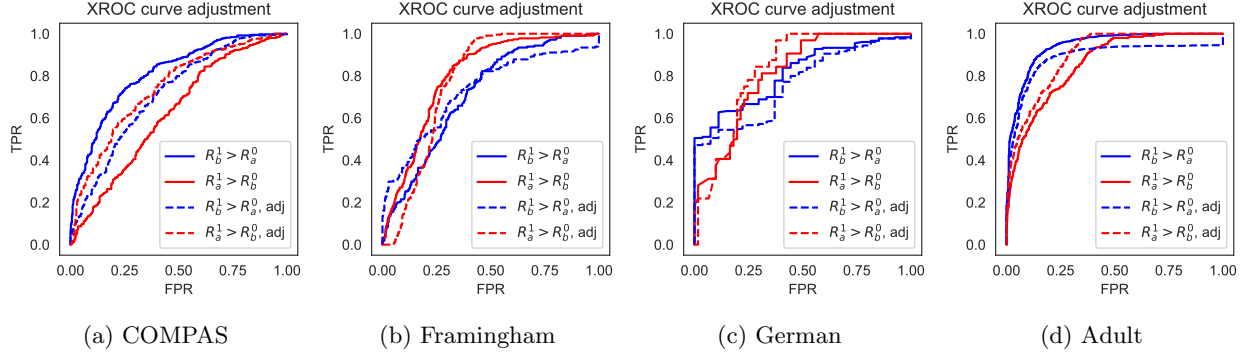


Figure 4: XROC curves, before and after adjustment

We might expect $\mu_{a_1} > \mu_{b_0}$ such that $\Pr[R_1^a > R_b^1] > \frac{1}{2}$. For a fixed mean discrepancy $\mu_{a_1} - \mu_{b_0}$ between the advantaged-guilty and disadvantaged-innocent (*e.g.*, in the COMPAS example), a decrease in variance increases the $\text{xAUC}(a, b)$. For fixed variance, an increase in the mean discrepancy $\mu_{b_1} - \mu_{a_0}$ increases xAUC . Thus, scores which are poor estimates of the Bayes-optimal score (therefore more uncertain) lead to higher xAUC s. Differences in the uncertainty across groups of these scores lead to xAUC disparities.

Note that the xAUC metric compares probabilities of misranking errors *conditional* on drawing instances from either $Y = 0$ or $Y = 1$ distribution. When base rates differ, interpreting this disparity as normatively problematic implicitly assumes *equipoise* in that we want random individuals drawn with equal probability from the white innocent/black innocent populations to face similar misranking risks, not drawn from the population distribution of offending.

Utility Allocation Interpretation When risk scores direct the expenditure of resources or benefits, we may interpret xAUC disparities as informative of group-level downstream utility disparities, if we expect resource or utility prioritizations which are *monotonic* in the score R . (We consider settings where we expect benefits for individuals to be non-decreasing in the expended resources $u(R)$, due to mechanistic knowledge.) In particular, allowing for any monotonic allocation u , the xAUC measures $\Pr[u(R_1^a) > u(R_b^b)]$. Disparities in this measure suggest greater probability of confusion in terms of less effective utility allocation between the positive and negative classes of different groups.

We can also consider the following integral representation of the xAUC disparities (*e.g.*, as in [32]) as differences between the *average rank* of positive examples from one group above negative examples from another group.

$$\begin{aligned} \Delta \text{xAUC} &= \mathbb{E}_{X_1^a} [F_0^b(R(X_1^a))] - \mathbb{E}_{X_1^b} [F_0^a(R(X_1^b))] \\ \Delta \text{xAUC}_0 &= \mathbb{E}_{X_1} [F_0^b(R(X_1)) - F_0^a(R(X_1))] \\ \Delta \text{xAUC}_1 &= \mathbb{E}_{X_1^a} [F_0(R(X_1^a))] - \mathbb{E}_{X_1^b} [F_0(R(X_1^b))] \end{aligned}$$

6.1 Adjusting Scores for Equal xAUC

We study the possibility of post-processing adjustments of a predicted risk score that yield equal xAUC across groups, noting that the exact nature of the problem domain may pose strong barriers to the implementability or individual fairness properties of post-processing adjustment.

Without loss of generality, we consider transformations $h : \mathbb{R} \mapsto \mathbb{R}$ on group b . When h is monotonic, the

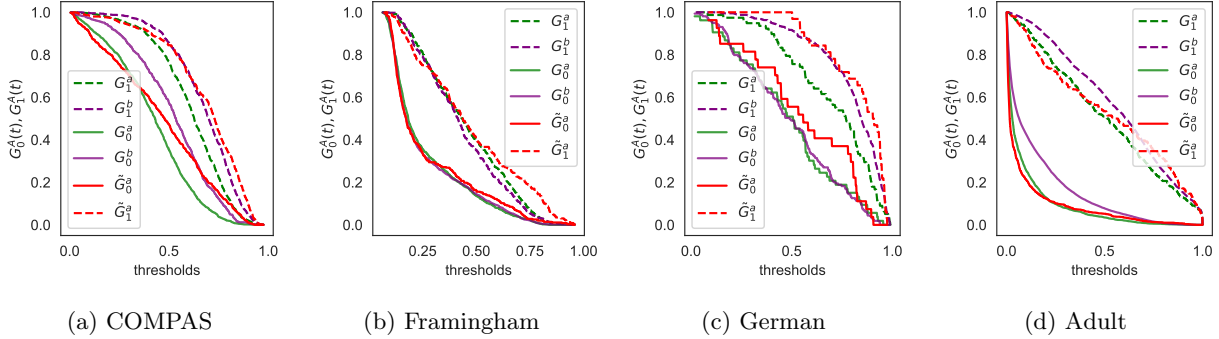


Figure 5: TPR and FPR curves over thresholds (G_y^a), and adjusted curves for group $A = a$ (\tilde{G}_y^a)

Table 2: Metrics before and after xAUC parametric adjustment

	COMPAS	Fram.	German	Adult
AUC (original)	0.743	0.771	0.798	0.905
AUC (adjusted)	0.730	0.772	0.779	0.902
α^*	4.70	3.20	4.71	4.43
xAUC(a, b)	0.724	0.761	0.753	0.895
xAUC(b, a)	0.716	0.758	0.760	0.898

within-group AUC is preserved.

$$\begin{aligned}
 \Pr[h(R_1^b) - R_0^a > 0] &= \Pr[R_1^a - h(R_0^b) > 0] \\
 &= \int G_1^b(h^{-1}((G_0^a)^{-1}(s)))ds = \int G_1^a(h((G_0^b)^{-1}(s)))ds
 \end{aligned}$$

Although solving analytically for the fixed point is difficult, empirically, we can simply optimize the xAUC disparity over parametrized classes of monotonic transformations h , such as the logistic transformation $h(\alpha, \beta) = \frac{1}{1 + \exp(-(\alpha x + \beta))}$. We can further restrict the strength of transformation by restricting the range of parameters.

In Fig. 4 we plot the unadjusted and adjusted xROC curves (dashed) resulting from a transformation which equalizes the xAUC; we transform group $A = a$, the disadvantaged group. We optimize the empirical xAUC disparity over the space of parameters $\alpha \in [0, 5]$, fixing the offset $b = -2$. In Fig. 5, we plot the complementary cdfs G_y^a corresponding to evaluating TPRs and FPRs over thresholds, as well as for the adjusted score (red). In table 2, we show the optimal parameters achieving the lowest xAUC disparity, which occurs with relatively little impact on the population AUC, although it reduces the xAUC(b, a) of the advantaged group.

6.2 Fair classification post-processing and the xAUC disparity

One might consider applying the post-processing adjustment of Hardt et al. [25], implementing the group-specific thresholds as group-specific shifts to the score distribution. Note that an equalized odds adjustment would equalize the TPR/FPR behavior for every threshold; since equalized odds might require randomization between two thresholds, there is no monotonic transform that equalizes the xROC curves for every thresholds.

We instead consider the reduction in xAUC disparity from applying the ‘‘equality of opportunity’’ adjustment that only equalizes TPR. For any specified true positive rate ρ , consider group-specific thresholds θ_a, θ_b achieving ρ . These thresholds satisfy that $G_1^a(\theta_a) = G_1^b(\theta_b)$. Then $\theta_b = (G_1^b)^{-1}(G_1^a(\theta_a))$. The score

transformation on R that achieves equal TPRs is:

$$h(r, A) = \begin{cases} r & \text{if } A = a \\ (G_1^a)^{-1}(G_1^b(r)) & \text{if } A = b \end{cases}$$

Proposition 4. *The corresponding xAUC under an equality of opportunity adjustment, where $\tilde{R}_{eqop} = h(R)$, is:*

$$\Delta \text{xAUC}(\tilde{R}_{eqop}) = \text{AUC}^b - \text{AUC}^a$$

Proof.

$$\begin{aligned} \Delta \text{xAUC}(\tilde{R}_{eqop}) &= \int G_1^a((G_1^a)^{-1}(G_1^b((G_0^b)^{-1}(s)))) ds \\ &\quad - \int G_1^b((G_1^b)^{-1}(G_1^a((G_0^a)^{-1}(s)))) ds \\ &= \int (G_1^b((G_0^b)^{-1}(s))) ds - \int G_1^a((G_0^a)^{-1}(s)) ds \\ &= \text{AUC}^b - \text{AUC}^a \end{aligned}$$

□

7 Conclusion

The xAUC metrics are intended to illustrate and help interpret the potential for disparate impact of predictive scores. The xROC curve and xAUC metrics provide insight on the disparities that may occur with the implementation of a predictive risk score in broader, but practically relevant settings, beyond binary classification.

References

- [1] S. Agarwal and D. Roth. Learnability of bipartite ranking functions. *Proceedings of the 18th Annual Conference on Learning Theory, 2005*, 2005.
- [2] J. Angwin, J. Larson, S. Mattu, and L. Kirchner. Machine bias. Online., May 2016.
- [3] C. Barabas, K. Dinakar, J. Ito, M. Virza, and J. Zittrain. Interventions over predictions: Reframing the ethical debate for actuarial risk assessment. *Proceedings of Machine Learning Research*, 2017.
- [4] S. Barocas and A. Selbst. Big data’s disparate impact. *California Law Review*, 2014.
- [5] J. Bonta and D. Andrews. Risk-need-responsivity model for offender assessment and rehabilitation. 2007.
- [6] G. W. Brier. Verification of forecasts expressed in terms of probability. *Monthly Weather Review*, 1950.
- [7] L. E. Celis, D. Straszak, and N. K. Vishnoi. Ranking with fairness constraints. *45th International Colloquium on Automata, Languages, and Programming (ICALP 2018)*, 2018.
- [8] C. Chan, G. Escobar, and J. Zubizarreta. Use of predictive risk scores for early admission to the icu. *MSOM*, 2018.
- [9] I. Chen, F. Johansson, and D. Sontag. Why is my classifier discriminatory? *In Advances in Neural Information Processing Systems 31*, 2018.

- [10] A. Chojnacki, C. Dai, A. Farahi, G. Shi, J. Webb, D. T. Zhang, J. Abernethy, and E. Schwartz. A data science approach to understanding residential water contamination in flint. *Proceedings of KDD 2017*, 2017.
- [11] A. Chouldechova. Fair prediction with disparate impact: A study of bias in recidivism prediction instruments. In *Proceedings of FATML*, 2016.
- [12] A. Chouldechova, E. Putnam-Hornstein, D. Benavides-Prado, O. Fialko, and R. Vaithianathan. A case study of algorithm-assisted decision making in child maltreatment hotline screening decisions. *Conference on Fairness, Accountability, and Transparency*, 2018.
- [13] S. Corbett-Davies and S. Goel. The measure and mismeasure of fairness: A critical review of fair machine learning. *ArXiv preprint*, 2018.
- [14] C. Cortes and M. Mohri. Confidence intervals for the area under the roc curve.
- [15] C. Cortes and M. Mohri. Auc optimization vs. error rate minimization. *Proceedings of the 16th International Conference on Neural Information Processing Systems*, 2003.
- [16] B. Cowgill. The impact of algorithms on judicial discretion: Evidence from regression discontinuities. *Working paper*, 2018.
- [17] D. Dheeru and E. K. Taniskidou. Uci machine learning repository. <http://archive.ics.uci.edu/ml>, 2017.
- [18] W. Dieterich, C. Mendoza, and T. Brennan. Compas risk scales: Demonstrating accuracy equity and predictive parity. *Technical Report*, 2016.
- [19] C. Dwork, M. Hardt, T. Pitassi, O. Reingold, and R. Zemel. Fairness through awareness. *Proceedings of the 3rd Innovations in Theoretical Computer Science Conference*, 2011.
- [20] Y. Freund, R. Iyer, R. Schapire, and Y. Singer. An efficient boosting algorithm for combining preferences. *Journal of Machine Learning Research 4 (2003)*, 2003.
- [21] S. Friedler, C. Scheidegger, S. Venkatasubramanian, S. Choudhary, E. P. Hamilton, and D. Roth. A comparative study of fairness-enhancing interventions in machine learning. *ACM Conference on Fairness, Accountability and Transparency (FAT*)*, 2019.
- [22] A. Fuster, P. Goldsmith-Pinkham, T. Ramadorai, and A. Walther. Predictably unequal? the effects of machine learning on credit markets. *SSRN:3072038*, 2018.
- [23] D. Hand. Measuring classifier performance: a coherent alternative to the area under the roc curve. *Machine Learning*, 2009.
- [24] J. Hanley and B. McNeil. The meaning and use of the area under a receiver operating characteristic (roc) curve. *Radiology*, 1982.
- [25] M. Hardt, E. Price, N. Srebro, et al. Equality of opportunity in supervised learning. In *Advances in Neural Information Processing Systems*, pages 3315–3323, 2016.
- [26] U. Hebert-Johnson, M. Kim, O. Reingold, and G. Rothblum. Multicalibration: Calibration for the (computationally-identifiable) masses. *Proceedings of the 35th International Conference on Machine Learning, PMLR 80:1939-1948*, 2018.
- [27] K. Holstein, J. W. Vaughan, H. D. III, M. Dudk, and H. Wallach. Improving fairness in machine learning systems: What do industry practitioners need? *2019 ACM CHI Conference on Human Factors in Computing Systems (CHI 2019)*, 2019.

- [28] J. Jones, N. Shah, C. Bruce, and W. F. Stewart. Meaningful use in practice: Using patient-specific risk in an electronic health record for shared decision making. *American Journal of Preventive Medicine*, 2011.
- [29] J. Kleinberg, S. Mullainathan, and M. Raghavan. Inherent trade-offs in the fair determination of risk scores. *To appear in Proceedings of Innovations in Theoretical Computer Science (ITCS), 2017*, 2017.
- [30] C. E. Kontokosta and B. Hong. Who calls for help? statistical evidence of disparities in citizen-government interactions using geo-spatial survey and 311 data from kansas city. *Bloomberg Data for Good Exchange Conference*, 2018.
- [31] L. Liu, M. Simchowitz, and M. Hardt. Group calibration is a byproduct of unconstrained learning. *ArXiv preprint*, 2018.
- [32] A. Menon and R. C. Williamson. Bipartite ranking: a risk-theoretic perspective. *Journal of Machine Learning Research*, 2016.
- [33] J. M. C. S. S. V. Michael Feldman, Sorelle Friedler. Certifying and removing disparate impact. *Proceedings of KDD 2015*, 2015.
- [34] M. Mohri, A. Rostamizadeh, and A. Talwalkar. *Foundations of Machine Learning*. 2012.
- [35] H. Narasimhan and S. Agarwal. On the relationship between binary classification, bipartite ranking, and binary class probability estimation. *Proceedings of NIPS 2013*, 2013.
- [36] A. Rajkomar, M. Hardt, M. D. Howell, G. Corrado, and M. H. Chin. Ensuring fairness in machine learning to advance health equity. *Annals of Internal Medicine*, 2018.
- [37] B. Reilly and A. Evans. Translating clinical research into clinical practice: Impact of using prediction rules to make decisions. *Annals of Internal Medicine*, 2006.
- [38] C. Rudin, R. J. Passonneau, A. Radeva, H. Dutta, SteveJerome, and D. Isaac. A process for predicting manhole events in manhattan. *Machine Learning*, 2010.
- [39] A. Singh and T. Joachims. Fairness of exposure in rankings. *Proceedings of KDD 2018*, 2018.
- [40] K. Yang and J. Stoyanovich. Measuring fairness in ranked outputs. *Proceedings of SSDBM 17*, 2017.
- [41] M. B. Zafar, I. Valera, M. G. Rodriguez, and K. P. Gummadi. Fairness beyond disparate treatment & disparate impact: Learning classification without disparate mistreatment. *Proceedings of WWW 2017*, 2017.

A Analysis

Proof of Lemma 2. For the sake of completeness we include the probabilistic derivation of the AUC, analogous to similar arguments for AUC [24, 23].

By a change of variables and observing that $\frac{d}{dv}G^{-1}(v) = -\frac{1}{G'(G^{-1}(v))} = \frac{1}{-f}$, if we consider the mapping between threshold s that achieves TPR v , $s = G^{-1}(v)$, we can rewrite the AUC integrated over the space of scores s as

$$\int_{-\infty}^{\infty} G_1^a(s) f_0^b(s) ds$$

Recalling the conditional score distributions $R_1^a = R \mid Y = 1, A = a$ and $R_0^b = R \mid Y = 0, A = b$, then the probabilistic interpretation of the AUC follows by observing

$$\begin{aligned} \int_{-\infty}^{\infty} G_1^a(s) f_0^b(s) ds &= \int_0^1 \Pr[R > s \mid Y = 1, A = a] \Pr[R = s \mid Y = 0] ds \\ &= \int_0^1 \left(\int_0^1 \mathbb{I}(R_1^a > s) \Pr[R_1^a = t] dt \right) \Pr[R_0^b = s] ds \\ &= \int_0^1 \int_0^1 \mathbb{I}(R_1^a > R_0^b) f_1^a(t) f_0^b(s) ds dt = \mathbb{E}[\mathbb{I}(R_1^a > R_0^b)] = \Pr[\mathbb{I}(R_1^a > R_0^b)] \end{aligned}$$

□

Proof of Proposition 3. We show this for the decomposition $\Pr[R_1 > R_0] = \sum_{a' \in \mathcal{A}} \Pr[A = a' \mid Y = 0] \Pr[R_1 > R_0^{a'}]$; the others follow by applying the same argument.

$$\begin{aligned} \sum_{a' \in \mathcal{A}} \Pr[A = a' \mid Y = 1] \Pr[R_1^{a'} > R_0] &= \sum_{a' \in \mathcal{A}} \Pr[A = a' \mid Y = 1] \int_r \Pr[R > r \mid A = a', Y = 1] \Pr[R_0 = r] dr \\ &= \sum_{a' \in \mathcal{A}} \int_r \Pr[R > r, A = a' \mid Y = 1] \Pr[R_0 = r] dr \\ &= \int_r \sum_{a' \in \mathcal{A}} \Pr[R > r, A = a' \mid Y = 1] \Pr[R_0 = r] dr \\ &= \int_r \Pr[R > r \mid Y = 1] \Pr[R_0 = r] dr = \Pr[R_1 > R_0] \end{aligned}$$

□

B Additional Empirics

B.1 Balanced xROC curves and score distributions

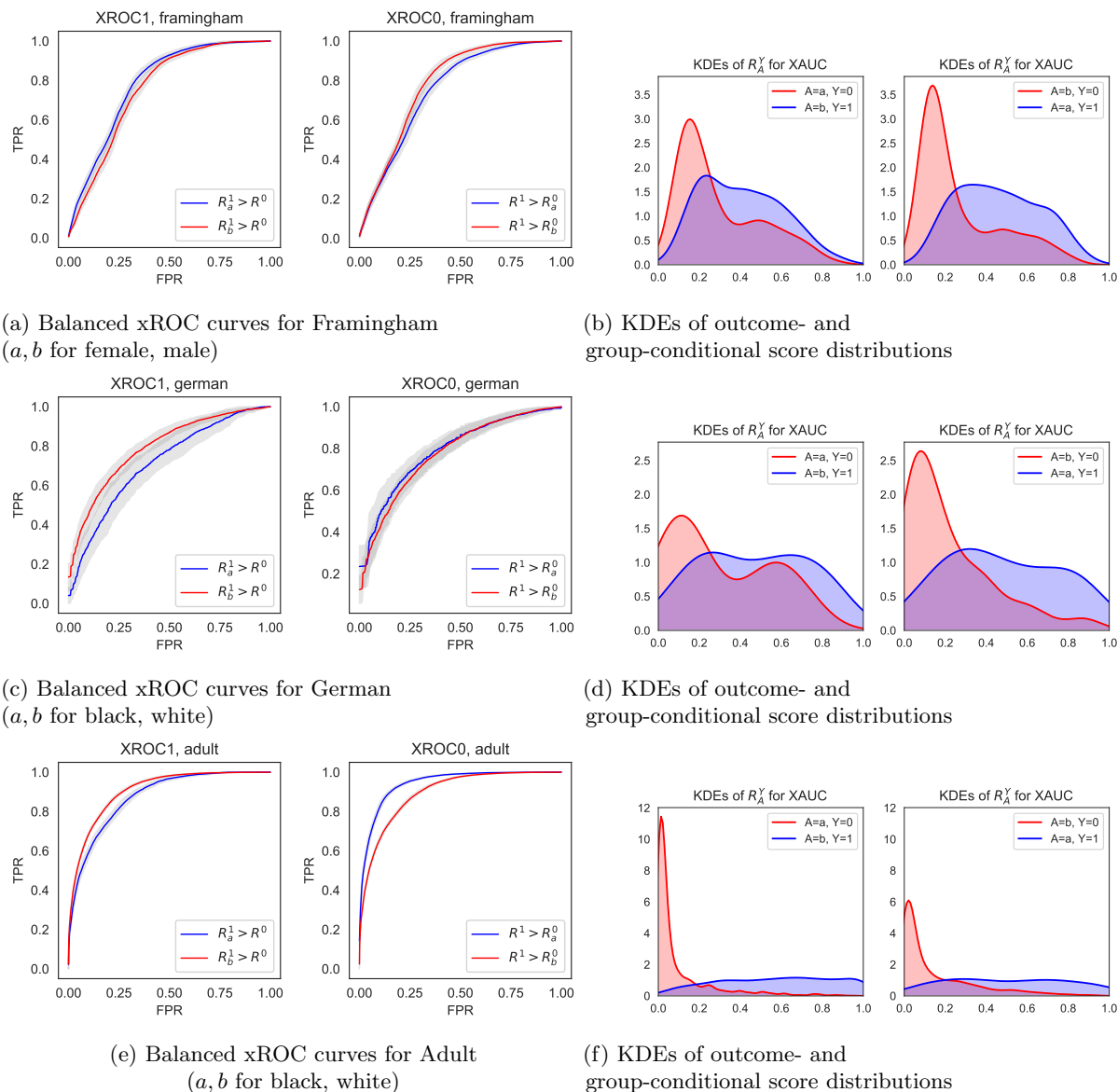


Figure 6: Comparison of balanced xROC curves for Framingham, German, and Adult datasets

We compute the similar xROC decomposition for all datasets. For Framingham and German, the balanced XROC decompositions do not suggest unequal ranking disparity burden on the innocent or guilty class in particular. For the Adult dataset, the xAUC_0 disparity is higher than the xAUC_1 disparity, suggesting that the misranking disparity is incurred by low-income whites who are spuriously recognized as high-income (and therefore might be disproportionately extended economic opportunity via *e.g.* favorable loan terms). The Framingham data is obtained from <http://biostat.mc.vanderbilt.edu/DataSets>.

Framingham, German, and Adult have more peaked distributions (more certain) for the $Y = 0$ class with more uniform distributions for the $Y = 1$ class; the adult income dataset exhibits the greatest contrast in

variance between the $Y = 0$ and $Y = 1$ class.

C Standard errors for reported metrics

Table 3: Standard errors of the metrics (AUC, xAUC, Brier scores for calibration) for different datasets by Logistic Regression (Log Reg.) and Rankboost, calibrated (RB, cal).

$A =$		COMPAS		Framingham		German		Adult	
		a	b	a	b	a	b	a	b
Log Reg.	AUC	0.011	0.018	0.016	0.014	0.049	0.029	0.007	0.004
	Brier	0.004	0.006	0.007	0.006	0.023	0.012	0.004	0.002
	XAUC	0.023	0.018	0.013	0.02	0.048	0.031	0.01	0.004
	XAUC ¹	0.012	0.015	0.012	0.014	0.044	0.024	0.009	0.003
	XAUC ⁰	0.012	0.019	0.015	0.012	0.032	0.029	0.004	0.004
RB, cal.	AUC	0.011	0.014	0.015	0.013	0.045	0.027	0.008	0.003
	Brier	0.004	0.005	0.005	0.004	0.022	0.009	0.003	0.002
	XAUC	0.025	0.016	0.012	0.017	0.044	0.031	0.01	0.004
	XAUC ¹	0.012	0.013	0.012	0.013	0.041	0.024	0.009	0.003
	XAUC ⁰	0.011	0.019	0.014	0.01	0.03	0.026	0.004	0.003